Proceedings of ASME Turbo Expo 2011
GT2011
June 6-10, 2011, Vancouver, British Columbia, Canada

GT2011-45218

SHIP PROPULSION SELF-EXCITED TORSIONAL VIBRATION

Glenn McAndrews
GE Marine
Cincinnati, OH, USA

Robert Murray
GE Global Research
Niskayuna, NY, USA

Paul Gemin
GE Global Research
Niskayuna, NY, USA

ABSTRACT

Self-excited vibration is demonstrated in many common day events, for example, wheel-castor shimmy or a traffic sign twisting in a steady strong wind [1]. Another example, blade flutter, is well known in the gas turbine community. The affected system will typically oscillate at its natural frequency. When applied to propulsion shafting, the phenomenon produces significant levels of alternating torque that negatively affects the reliability of the drivetrain hardware.

Starting with basic principles, this paper examines the conditions that can lead to self-excited torsional vibration. A screening parameter is developed that can be used to evaluate the potential for system instability. System stability mapping results are presented showing the effect of basic input parameters such as inertia, stiffness, and damping.

The potential for self-excited torsional vibration is discussed in the context of recent trends in marine gas turbine propulsion (e.g. lightweight propulsors). Finally, countermeasures using the engine control system are outlined.

INTRODUCTION

Shipbuilders will often perform or contract a torsional vibration analysis for the purpose of identifying the mode shapes, frequencies, and levels of alternating torque. When torsional vibration problems do arise, and they are not predicted by the analysis, then it is reasonable to ask - what is wrong with the analysis or more appropriately, are there limitations in a conventional analysis that fail to forecast non-conventional behaviors. Such is the case in the event described herein.

The primary author recently was part of an industry team that faced a shipboard torsional vibration problem that affected the gas turbine drive train. The oscillation had characteristics that at the time appeared unique and novel, even to most experienced industry participants onboard. For the purposes of this discussion, a simplified sketch of the drivetrain is shown in Figure 1. The drivetrain is fairly straight-forward, so the likelihood of anomalies would seem remote.

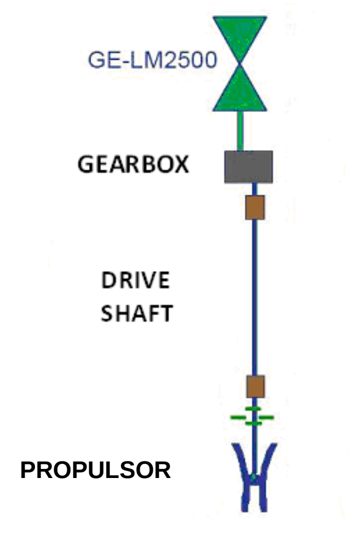

FIGURE 1 – PROPULSION PLANT CONFIGURATION

PROBLEM DESCRIPTION

During initial sea trials it was discovered that under certain operating conditions (ship speed, maneuvering, shaft horsepower) the gas turbine drivetrain exhibited a dynamic instability marked by a dramatic oscillation in shaft output speed/torque. Upon inspection of Figure 2, it was originally thought that gas turbine engine control dynamics were somehow at fault.

In this graph, where:

NPT = free power turbine output speed (rpm)

it is indeed true that the fuel valve participated in the event. However detailed analysis of the gas turbine parameters revealed that the fuel valve was following the load and not leading it. This is not surprising for a turbine operating on a NPT speed/accel closed-loop regulator as was the case here.

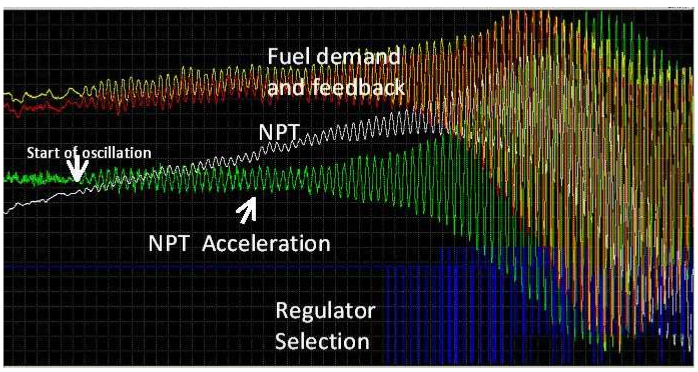

FIGURE 2 – INSTABILITY EVENT ON NPT SPEED CONTROL

As proof that something other than the engine control was contributing to the instability, the engine control was put into “core speed control”, whereby the power turbine speed “floats” with changes in load and the gas generator power output stays constant. The oscillation event was repeated and the results are shown in Figure 3. It was demonstrated that all the gas turbine parameters (core speed, fuel manifold pressure, fuel valve position) remained constant but the output speed, in white, still oscillated wildly about some nominal value (NPT acceleration in purple).

ALTERNATING TORQUE

Most readers will recognize that torsional vibrations such as the one described herein have negative effects on the reliability of the affected components. Fatigue results from the large alternating stresses. It becomes necessary therefore to evaluate the level of the alternating torque at a given location. Although what follows was performed by the authors to evaluate power turbine torque, the same approach could be used for any component in the drive train.

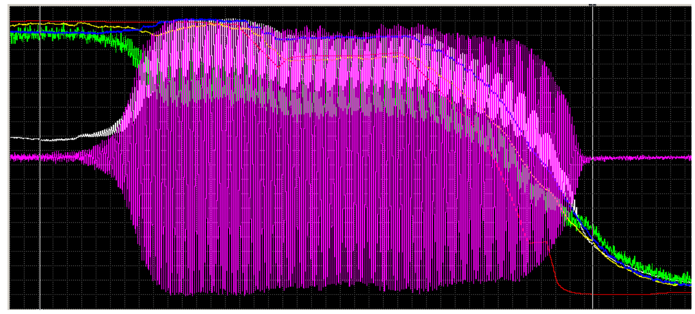

FIGURE 3 – INSTABILITY EVENT ON CORE SPEED CONTROL

The alternating torque in the free power turbine shaft is calculated from the following relation:

$$T = J_p \, \alpha \qquad (1)$$

Where T= torque
Jp = polar moment of inertia of the PT
α = angular acceleration

The angular acceleration was obtained by analyzing PT speed signal data from Figure 3 as follows:

$$\alpha = \omega \, \Omega \qquad (2)$$

where ω = frequency of the speed oscillation
Ω = peak variation in the NPT speed

Using this approach, alternating torque values of roughly 40% of the maximum torque were computed. A level of 10% or below is generally considered a good benchmark for satisfactory performance.

PROBLEM RESOLUTION

As a first step, the drive-train torsional vibration analysis report was examined. Notably, the observed oscillation frequency of 6 Hz closely matched the prediction of the system’s primary natural frequency. At this point, the classical vibration problem was framed – “what is exciting the first torsional mode?” Additional data collection did not reveal an obvious excitation source, although it was generally accepted that the oscillation coincided with the onset of propulsor cavitation. Cavitation therefore seemed to contribute to the problem but lacked the necessary “energy credentials” to be considered an excitation source. The authors concluded that the oscillation had all the attributes of being a non-linear self-excited vibration, namely a vibration whose excitation is derived from the motion of the system, and is often initiated by “negative damping”, meaning the system damping decreases with increasing velocity.

The acceptance of this root cause possibility is hugely important because it leads to accepting some potential solutions and dismissing others. Forced resonance and self-excited instability are two distinct classes of vibration. Forced resonance requires *external excitation* and grows *linearly*, not exponentially as in the case of instability. Also, in a resonance, the frequency of the external excitation coincides with one of the system's natural frequencies. The remedy may include eliminating the excitation source. A self-excited instability does not require an excitation source and therefore the remedial action must be something other than eliminating the excitation. That leaves two equally valid choices. The first involves changing one or more of the key vibration inputs: mass, stiffness, or damping of the drivetrain components (e.g. adding a viscous damper). The second involves using the engine controller to detect and prevent occurrence. Before examining GE's control approach, it will be useful to understand the physics of this phenomenon and where it has surfaced in other industries.

SELF-EXCITED OSCILLATION

Kemper's experimental work [2] is one of the earliest papers written on the topic of self-excited torsional vibration. Kemper points out that there are two classes of self-excited behaviors, namely, *self-oscillation of the first kind*, wherein the motion consists of alternate sticking and slipping, and *self-oscillation of the second kind*, wherein the mass oscillates but does not come to a full stop. The open literature abounds with articles written about the first kind. Unfortunately the same cannot be said for the second kind.

Although several industries have produced publications outlining their approach to curing self-excited shafting oscillations, the "bloom" shown in Figure 3 is probably most familiar to professionals in the oil-drilling and the locomotive industries [3][4]. It is not surprising that the oil drilling industry would succumb to torsional vibration issues considering that drill strings are hundreds (even thousands) of meters in length. Likewise, it is not hard to envision a highly torqued locomotive wheel set violently "chattering" if were to happen upon some wet leaves across its tracks.

Further inspection of the oil industry literature reveals the not so surprising result that two solutions have successfully been employed in that field. One solution is based on changing the mechanical vibration properties at the drill head (damping). The other solution involves various degrees of motor control complexity, all of them designed to vary the electrical motor output in response to some monitored drilling parameter. The industry has successfully developed *active* dampening, whose net effect on the nominal output torque is zero (only the "AC component" is eliminated).

It has been suggested that control solutions limit process capability by reducing input power. In oscillating conditions however, it is often a torque breakdown (in our case from cavitation) that causes the instability and so the action to *temporarily* reduce input torque is a rational choice. The input torque can be thought of as being "transiently excessive" for the prevailing conditions.

Whether it's a propulsion drive train, oil drilling platform, or locomotive wheel set, researchers model the system as a torsional pendulum – the subject of our next section.

SYSTEM MODEL

For illustrating the physics, we start with a simple single mass torsional pendulum supported by a bearing. The model of Figure 4 was extensively studied by Kemper. Opposing the rotation, ω, is a bearing friction force, ***f***, whose coefficient, μ , follows the classical model:

$$\mu_{static} > \mu_{moving} \text{ and } \mu_{moving}(\omega) = \text{ constant} \tag{3}$$

For the rotating system, the equation of motion is:

$$J\ddot{\phi} + c(\dot{\phi} - \dot{\phi}_{initial}) + k(\phi - \phi_{initial}) = -f_{moving} \tag{4}$$

where ***c***, is the internal damping coefficient and

$$\dot{\phi}_{initial} = \omega \tag{5}$$

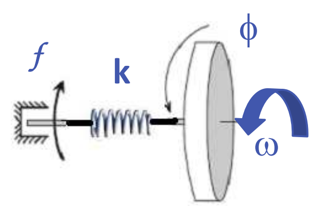

FIGURE 4 – SIMPLE PENDULUM MODEL

In this case, the system's negative damping characteristic results from nature of solid friction, whereby the friction torque decreases with increasing speed. Thus at time = zero, the shaft will twist an initial amount equal to $\boldsymbol{f}_{static}/k$. Breaking free, the friction force is decreased and oscillation will occur. Both analytically and experimentally, Kemper demonstrates that for this classical friction model, *sustained* self-excited oscillations of the first kind, will occur provided the rotational speed is ***below*** a critical value. In other words, at higher speeds, the rotor's relative velocity is never allowed to reach zero (allowing the rotor to stop with a resulting increase in friction).

For high speed turbomachinery and propulsors, stick-slip behavior is of little interest. But as Kemper suggests, one can analytically explore self-excited behavior of the second kind, by using the same mathematical model with a hypothetical friction curve that, for high speeds, contains a negative characteristic.

DERIVATION OF CRITICAL OSCILLATION PARAMETER FOR LARGE-SCALE MARITIME PROPULSION

Turning now to the LM2500 propulsion system of Figure 1, it is more appropriate to use a double mass pendulum separated by a long shaft. The resulting vibration model is shown in Figure 6. The negative damping characteristic results from waterjet torque reduction when waterjet shaft speed exceeds some critical value.

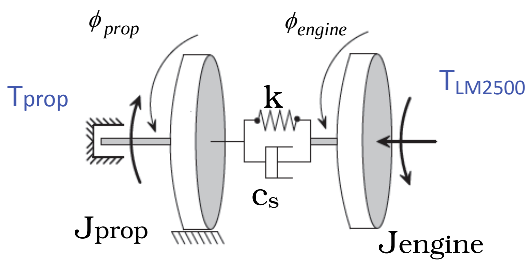

FIGURE 6 – PROPULSION TORSION MODEL

The torque reduction derives from the development of large-scale two-phase flow across the waterjet impeller (Zone 3 cavitation). Figure 7 provides some insight on the level of torque reduction associated with Zone 3 levels of cavitation. 3% reduction is typically used to define the critical suction specific speed for a pump, although a range of 2-5% has also been used [5].

The dynamics of a general drive-train are modeled here as lumped rotating masses on each end of a flexible shaft. The linear properties of the shaft are included via a spring constant

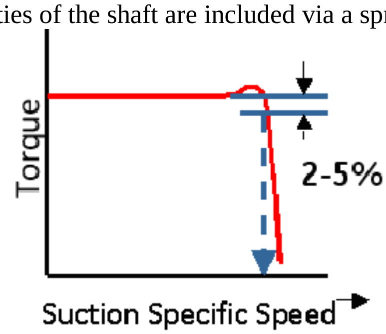

FIGURE 7 – TORQUE BREAKDOWN IN CAVITATION

and damping. The torques exerted at each end of the shaft (e.g. engine torque, hydrodynamic forces, bearing friction, gear friction, etc.) are included as T_{prop} and T_{engine} which can be determined and included as required.

$$J_{prop}\ddot{\phi}_{prop} = c_s\left(\dot{\phi}_{engine} - \dot{\phi}_{prop}\right) + k\left(\phi_{engine} - \phi_{prop}\right) - T_{prop}\left(\dot{\phi}_{prop}, t, \ldots\right) \tag{6}$$

$$J_{engine}\ddot{\phi}_{engine} = c_s\left(\dot{\phi}_{prop} - \dot{\phi}_{engine}\right) + k\left(\phi_{prop} - \phi_{engine}\right) + T_{engine}\left(\dot{\phi}_{engine}, t, \ldots\right) \tag{7}$$

Where J_{prop} and J_{engine} are the effective moments of inertia of the prop (propulsor unit) and of the lumped motor & transmission, c_s is the damping coefficient of the coupling shaft, k is the spring-constant of the shaft, and ϕ_{prop} and ϕ_{engine} are the angular positions of the prop and of the transmission output respectively. Here the power source (LM2500) and the transmission are lumped together as a single 'stiff' unit. The torques applied at each end (T_{prop} and T_{engine}) use a sign convention such that each is positive in its typical direction. The torque from the prop end of the shaft, $T_{prop,}$ and from the engine end of the shaft, $T_{engine,}$ will be free to be calculated at each time step. Presumably, without accounting for bearing losses or gear friction, T_{engine} will be equal to nT_{LM2500}, where n is the gear ratio of the transmission. As presented, there is no friction at each end of the shaft, only friction in the relative motion between the two ends, in the shaft. However, if desired, friction can be added at each end of the shaft by simple modification of T_{fluid} and T_{engine}. Additional insight can be found by algebraic manipulation of Equations 6 and 7 and changing variables to yield the following two *independent* equations of motion.

$$J_{red}\ddot{\theta} + c_s\dot{\theta} + k\theta + \left(\frac{J_{engine}T_{prop} + J_{prop}T_{engine}}{J_{prop} + J_{engine}}\right) = 0 \tag{8}$$

$$\left(J_{prop}\ddot{\phi}_{prop} + J_{engine}\ddot{\phi}_{engine}\right) + \left(T_{prop} - T_{engine}\right) = 0 \tag{9}$$

Where, entirely analogous to a reduced-mass system in linear motion, the reduced moment of inertia and shaft twist variable are defined as follows. A slight distinction from the norm here is that external forces are applied, as opposed to forces between the two bodies as in orbital motion for instance.

$$J_{red} = \frac{J_{prop}J_{engine}}{J_{prop} + J_{engine}} \tag{10}$$

$$\theta = \phi_{prop} - \phi_{engine} \tag{11}$$

In a sense, Equation 9 represents the desired dynamics of the system, a balance between the engine torque, the propeller (or water jet) torque, and the inertia of the system. Drive-train oscillation is governed by Equation 8.

CONDITIONS FOR SELF-EXCITED OSCILLATION

Consider, as a starting point, that the drivetrain conditions are 'steady'. By this we mean that vehicle velocity, torque, throttle input, etc. are not changing significantly over a time-period of the natural resonance of the drive-train.

We will neglect time dependent aspects of cavitation and engine dynamics and make the assumption that changes in the torque exerted by the power train, and by the propeller/water-jet are functions of their respective rotation rates, and not of other time dependent effects. For small deviations, from steady values, we will assume a linear dependence between torque and rotation rate, i.e.

$$T_{prop} = T_{prop,steady} - \dot{\phi}_{prop,unsteady}\, c_{prop} = 0 \qquad (12)$$

$$T_{engine} = T_{engine,steady} - \dot{\phi}_{engine,unsteady}\, c_{engine} = 0 \qquad (13)$$

The constants c_{prop} and c_{engine} are then equal to the negative of the slope of the torque versus rpm curve of the prop and engine respectively. The final step is to assess the effect of a perturbation to the system. In particular, we will search for conditions and criteria in which a small oscillation will grow, as opposed to decay back to steady values. Using the equations of motion, we will show how each end of the drivetrain responds to perturbation, and when the balance of shaft-twist and external torques amplifies an oscillation, or dampens it.

ASSUMPTIONS AND DEVELOPMENT OF PERTURBATION/UNSTEADY MODEL

To begin, time derivatives of steady terms are set to zero (relative to time derivatives of fluctuating terms)

$$\begin{aligned}\ddot{\phi}_{prop} &= \ddot{\phi}_{prop,unsteady}\\ \ddot{\phi}_{engine} &= \ddot{\phi}_{engine,unsteady}\end{aligned} \qquad (14)$$

Consider Equation 9 under the 'steady' condition outlined above. In this case, it is permissible for the vessel to be under hard acceleration, however, the drivetrain has already accelerated to its equilibrium rotation rate at the current vessel speed. To elaborate more, when a new throttle position is set, the drivetrain will quickly respond and accelerate to a new point. After this, the vessel slowly accelerates and the drivetrain slowly changes with the vehicle speed. This latter process is typically slow with respect to drivetrain oscillation and can be considered steady, as defined above. Equation 9 is then set to zero, and can be integrated readily.

$$T_{prop,steady} - T_{engine,steady} = 0 \qquad (15)$$

$$\begin{aligned}&\left(J_{prop}\ddot{\phi}_{prop,unsteady} + J_{engine}\ddot{\phi}_{engine,unsteady}\right) + \\ &\left(T_{prop,unsteady} - T_{engine,unsteady}\right) = 0\end{aligned} \qquad (16)$$

Because we are looking to understand how the system will deviate from steady condition, we can integrate the above, and use steady conditions (unsteady terms = zero) as the starting point.

$$\begin{aligned}&\int_{steady}^{unsteady}\left(J_{prop}\ddot{\phi}_{prop,unsteady} + J_{engine}\ddot{\phi}_{engine,unsteady}\right) + \left(T_{prop,unsteady} - T_{engine,unsteady}\right)dt\\ &= \left(J_{prop}\dot{\phi}_{prop,unsteady} + J_{engine}\dot{\phi}_{engine,unsteady}\right) + \int_{steady}^{unsteady}\left(T_{prop,unsteady} - T_{engine,unsteady}\right)dt\\ &= 0\end{aligned} \qquad (17)$$

Note that the steady conditions in Equation 17 were the same in the lower and upper bounds of the integral and subtracted out. Next, note that we are looking for slowly growing disturbances, or at the very least, we are seeking the critical conditions at which disturbances are slowly amplified. In such a case, entirely analogous to pushing a child on a swing, the amplitude of the momentum oscillating back and forth in the system (left side of Equation 17), is considerably greater than the cycle-to-cycle forcing term that is slowly adding to the momentum each cycle (right side of Equation 17). Also note that the forcing term integrates back to zero in each cycle. For the purpose of finding the critical stability parameter, we will then neglect the effects of the right side of Equation 17. If precise amplitudes of oscillation and rates of increase are required, then this can be revisited.

$$J_{prop}\dot{\phi}_{prop,unsteady} + J_{engine}\dot{\phi}_{engine,unsteady} = 0 \qquad (18)$$

With all the qualification and description leading up to Equation 18, it turns out to be equivalent to conservation of angular momentum in the absence of external forces. It would appear the assumptions of 'steady' conditions could be equivalent to stating that changes to the angular momentum of the drivetrain are small over an oscillation period.

PARAMETER DERIVATION

Equations 11 and 18 can be solved algebraically for the unsteady rotation rates at each end.

$$\dot{\phi}_{prop,unsteady} = \frac{J_{engine}}{J_{prop} + J_{engine}}\dot{\theta} \qquad (19)$$

$$\dot{\phi}_{engine,unsteady} = -\frac{J_{prop}}{J_{prop} + J_{engine}}\dot{\theta} \qquad (20)$$

We now have sufficient information to determine the effect of small perturbations to the system. Substituting Equations 19 and 20 into Equation 12 and 13, then back into Equation 8, results in the following equation,

$$J_{red}\left(\ddot{\theta}\right)+c_s\left(\dot{\theta}\right)+k\left(\theta\right)+$$
$$\frac{J_{engine}}{J_{prop}+J_{engine}}\left(T_{prop,steady}-\frac{J_{red}}{J_{prop}}\dot{\theta}\ c_{prop}\right)+$$
$$\frac{J_{prop}}{J_{prop}+J_{engine}}\left(T_{engine,steady}+\frac{J_{red}}{J_{prop}}\dot{\theta}\ c_{engine}\right)=0 \tag{21}$$

$$J_{red}\left(\ddot{\theta}\right)+c_{system}\left(\dot{\theta}\right)+k\left(\theta\right)+$$
$$\left[\frac{J_{red}}{J_{prop}}\left(T_{prop,steady}\right)+\frac{J_{red}}{J_{engine}}\left(T_{engine,steady}\right)\right]=0 \tag{22}$$

where the stability parameter for the system is,

$$c_{system}=c_s-\left(\frac{J_{red}}{J_{prop}}\right)^2 c_{prop}+\left(\frac{J_{red}}{J_{engine}}\right)^2 c_{engine}$$
$$=c_s-\left(\frac{J_{engine}}{J_{prop}+J_{engine}}\right)^2 c_{prop}+\left(\frac{J_{prop}}{J_{prop}+J_{engine}}\right)^2 n\, c_{LM2500} \tag{23}$$

Equation 22 represents the shaft-twist response to a perturbation. The main assumptions are that the torques at each end of the shaft are determined by the rotation rate (other sources of variation are neglected), and variation in rotation rates are small over a resonant period of the system. The negative rate of change of torque generated by the LM2500 with its rotation rate is then c_{LM2500}, and similarly, the negative rate of change of torque of the prop/water-jet with rotation rate is c_{prop}. These effective damping constants can be taken from the negative of the slope of the torque versus rpm curve for each device, at the operating point being investigated.

As a linear oscillator, the solution to Equation 22 is classically set forth as the sum of the homogenous solution (ring down from initial conditions) and the particular solution due to forcing. The homogenous solution is given as:

$$\theta_h = e^{-\frac{c_{system}}{2J_{red}}}\left[A\cos\left(2\pi f_{res}t\right)+B\sin\left(2\pi f_{res}t\right)\right]=0 \tag{24}$$

DISCUSSION

The conclusion to be drawn is that if the effective damping of the system (c_{system}) is negative, then oscillations at the natural frequency of the system will grow (ring-up as opposed to ring-down). The system damping put forth in Equation 23, and its result in Equation 24, are not entirely unexpected: the damping of the shaft is expected, damping due to the prop is expected if the prop torque increases with rotation rate, and damping due to the power source would be expected if torque reduces with increasing rotation rate. If the net effect of these swings in the wrong direction, then perturbations at the natural frequency are amplified.

As the governing condition for stability of the system, Equation 23 will be discussed further. If the damping coefficient of the coupling shaft is small ($c_s << c_e, c_p$), and if the damping coefficient of the engine is positive, i.e., the engine torque tends to decrease with increasing speed (a typical case, in particular if the control algorithm can respond at the resonant frequency), then the stability condition can be reduced to the following:

$$J_{prop} > \sqrt{\frac{c_{prop}}{c_{engine}}}\ J_{engine} \tag{25}$$

or

$$c_{engine} > \left(\frac{J_{engine}}{J_{prop}}\right)^2 c_{prop} \tag{26}$$

From Equation 25, we can see that, in regards to the system model developed here, the primary consideration for the ship designer is the ratio of inertias of the prime mover and driven equipment. With studies still in progress, the effect of shaft stiffness plays a lesser role, but as one might expect, higher stiffness is in the direction of improved stability.

PROPELLERS VERSUS WATER JETS

It is interesting to note that while there tends to be much focus on the negative damping effects of cavitation, the damping and inertial effects of the engine, at the other end of the drivetrain, are of comparable importance. The shift to lighter waterjets for propulsion should be assessed in terms of Equation 25 to ensure that the combination of engine and gearing inertia is not too far toward instability.

Table 1 – TYPICAL DRIVETRAIN PROPERTIES

	Propulsor Inertia (J1) kgm2	Shaftline stiffness Nm/rad	Prime Mover/GB (J2) inertia kgm2	Calculated Natural Frequency (Hz)
Waterjet ship	2000	2.37E+06	10000	6
Propeller ship	20000	2.11E+08	5000	36.5

With equations in hand, system stability mapping is facilitated by MATLAB or equivalent simulation tools. Figure 8 shows a representative stability boundary. Systems, such as those in Table 1, were examined applying Figure 9 as a cavitation model. Markers on the plot indicate points where the stability criteria were verified with the system model. Green points were stable, red unstable.

ENGINE CONTROL LOGIC – DETECT & PREVENT

It should be obvious that once at sea, not much can be done to address the problem, other than a control solution. Along those lines, GE developed NPT Dynamic Instability Protection Logic (NPTDIP) software to automatically detect and respond to NPT speed oscillations. Referring to Figure 11, the software resides in the Micronet® engine controller provided by Woodward. To prevent oscillation, energy is removed from the system by cutting back on engine fuel valve.

Detecting an oscillation requires using the engine speed signal in a manner that adequately discriminates an undesirable oscillation from other potential (and desirable) engine transients.

Referring to Figure 12, if one were to closely examine a portion of the speed signal during oscillation event, one cycle of oscillation would span approximately 167 milliseconds. The waveform can be thought of as having a “DC component” representing the mean value, and an “AC component” representing the variation around the mean.

The detection logic processes every 40 ms, creating NPT “samples” (power turbine speed in rpm) every 40 ms. Four representative speed samples taken at times: 160, 120, 80, 40, and 0 are illustrated in Figure 12. The detection logic subtracts each speed sample from the value taken 40 ms earlier. The

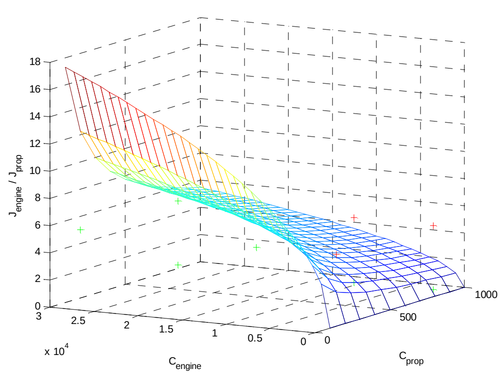

FIGURE 8 –STABILITY MAP

absolute value is taken for each delta. The four absolute values are then added together. The sum is multiplied by 6.25 (1000ms/160ms) in order to create an rpm/sec parameter called NPT_TOT_COMP. Every 40 ms NPT is simultaneously passing through a “rectifier function” whose net output, NPT_DC_COMP is the DC component of the sinusoid.

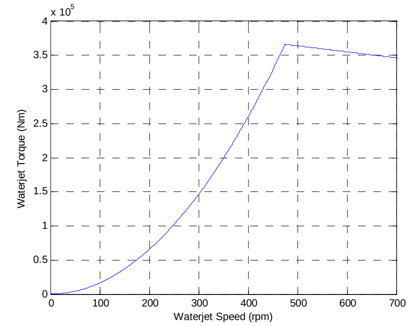

FIGURE 9 –CAVITATION MODEL

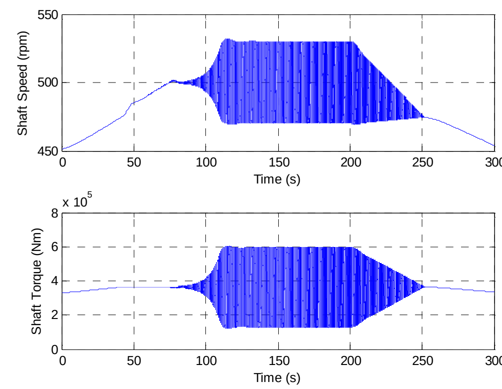

FIGURE 10 – SIMULATION EXAMPLE

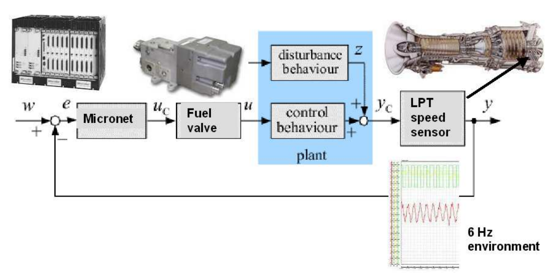

FIGURE 11 – ENGINE CONTROL SYSTEM

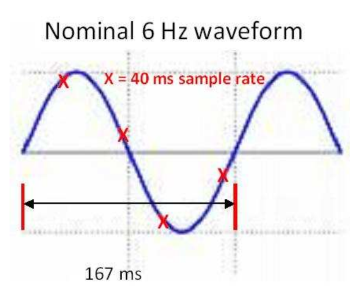

FIGURE 12 – TYPICAL SINUSOID

Knowing both the NPT_TOT_COMP and the NPT_DC_COMP the detection logic subtracts one from the other, yielding a control parameter named NPT_AC_COMP.

Figure 13 shows NPT_AC_COMP (in purple) during an oscillation event. In this figure, NPT_AC_COMP is being compared against the root mean square value of the power turbine acceleration signal, NPTRMS, shown in blue (NPTRMS having been an earlier detection method). When the NPT_AC_COMP value exceeds an adjustable threshold, the oscillation event is declared TRUE. If the event is declared true, a PI (proportional, integral) regulator acts as a topping governor, in effect, creating "anti-slip traction control". The PI regulator adjusts fuel flow to minimize the error signal created by NPT_AC_COMP and some user defined acceptable limit.

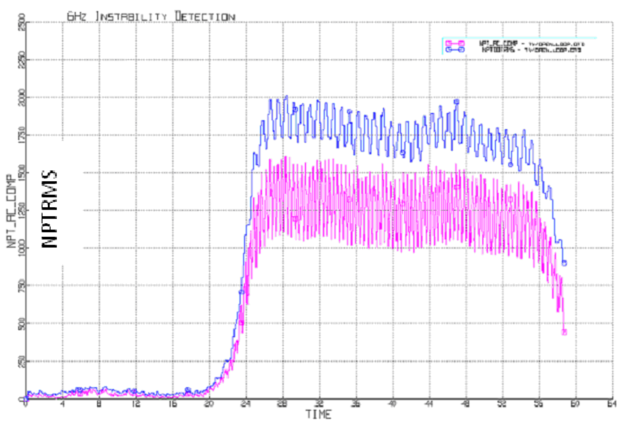

FIGURE 13 – DETECTION PARAMETERS

The NPTDIP logic proved very effective in the detection and prevention of the oscillation. Although a control solution does not eliminate the vibration conditions that can produce self-excited behavior, it helps to protect the machinery.

Figure 14 is a time plot of gas turbine parameters during a typical oscillation event; in this particular case, a full plant high speed turn. Of interest are the three colored lines:

Blue = gas generator core speed, rpm
Yellow = power turbine speed, rpm
Red = NPT_AC_COMP

The Figure's insert shows a close-up of the power turbine speed, clearly showing the onset of oscillation and its immediate abatement; the result of quick reductions in fuel flow. The loss of power/torque throughout the maneuver is surprisingly small, generally 0-5% depending on the kind of maneuver.

SUMMARY

Under the assumptions presented here, essentially a solid propulsor and a solid engine coupled by a flexible shaft, with the torques at each end being functions of their respective rotations rates, a stability parameter can be derived that depends upon the slopes of the torque-versus-rpm curves of the engine and of the propulsor, and also the rotational inertias of the engine and propulsor. Depending upon the sign of the derived stability parameter, small oscillations will either grow, or decay. This is a necessary condition for growing oscillations but the authors suspect it is not sufficient. The condition would indicate that propulsors and gearboxes of similar inertia are required to ensure oscillation do not occur. This is likely not practical with advanced propulsors and modern ship design. The shipbuilder can still design a lightweight propulsion system and should oscillations occur, a turbine control technique as describe in this paper enables smooth ship operation.

Having already impacted an existing ship class, self-excited torsional vibration and its significance for propulsion design warrants further research. Industry standards/guidelines may need to consider the outcome of this work.

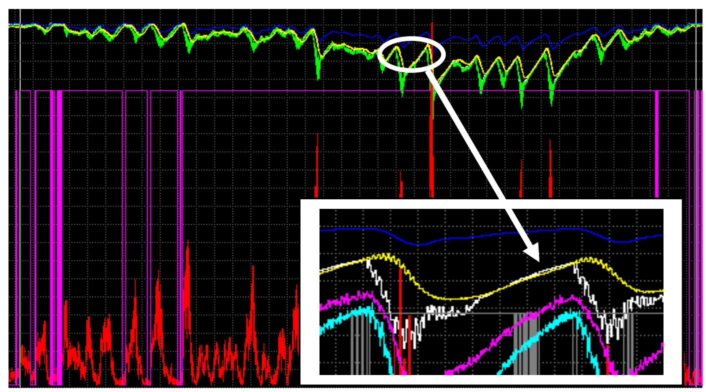

FIGURE 14 – Time Plot – "NPTDIP in action"

ACKNOWLEDGMENTS

The authors appreciate the support of their respective managers and specially thank GE's Art Radun for his mathematical and simulation contributions. Finally, Woodward's John Sterns was a key resource aboard the vessel.

REFERENCES

[1] Tse, F.S., Morse I.E., Hinkle R.T., Mechanical Vibration – Theory and Applications, 2nd ed. Chapter 8, pp.300, 321-323.
[2] J.D. Kemper, July 1966, "A Study of System Parameters Affecting Self-excited Torsional Oscillations" Experimental Mechanics.
[3] J. H Yu, T.X. Mei, and D.A. Wilson, 2006. "Re-adhesion control based on wheel set dynamics in railway traction system" University of Leeds.
[4] J.D. Jansen, L. van den Steen, 1995, "Active Damping of Self-Excited Torsional Vibrations in Oil Well Drill-strings" Journal of Sound and Vibration.
[5] Specialist Committee on Cavitation, 2008 Proceedings of the 25th ITTC, Fukuoka Japan.